INTERACTION TIMES OF HOMOGENEOUS AND HETEROGENEOUS DROPLETS IN GASES

by

Maxim PISKUNOV**, Nikita SHLEGEL, Svetlana KRALINOVA, Pavel TKACHENKO, and Olga VYSOKOMORNAYA

National Research Tomsk Polytechnic University, Tomsk, Russia

Original scientific paper
https://doi.org/10.2298/TSCI190928187P

In this research, we present the results of experiments measuring the interaction times of colliding liquid droplets in different modes (bounce, coalescence, separation, and disruption). The experiments involve water and typical water-based slurries, emulsions, and solutions. The main experimental parameters are close to those of high potential gas-vapor-droplet technologies (heat and mass transfer power plants, thermal and flame water treatment systems, and fuel technologies): droplet size 0.1-5 mm, velocities 0.1-10 m/s, liquid temperature 20-80 °C, impact angle 0-90°, and relative volume and mass fractions of liquid and solid additives in water 0-10%. We explore how a set of parameters and effects influence the characteristics of the processes under study. The most important of these parameters are relative droplet velocity, impact angle, impact parameter, and temperature. Using dimensionless linear and angular interaction parameters as well as the Weber, Reynolds, and Ohnesorge numbers, we produce interaction mode maps to consider the correlation of the main forces: inertia, surface tension, and viscosity. We determine the interaction times, number, size, and total surface area of the newly formed post-collision droplets and obtain approximations for the experimentally determined functions.

Key words: *droplet, coalescence, bounce, separation, disruption, interaction time*

Introduction

Specialized spraying – controlled, large-scale, and quite rapid atomization – of liquids, solutions, emulsions, and slurries is often used in typical technologies to improve evaporation, intensify fuel ignition and burnout, reduce anthropogenic emissions, cover larger areas by irrigation*, etc.* [1-4]. Several spraying technologies are now widespread [5, 6]: hydraulic, centrifugal, mechanical, pneumatic, acoustic, and compound (complex geometry of spraying systems; a set of nozzles at different angles with respect to each other; collision of the liquid with different targets*, etc.*). In each of the aforementioned technologies, a reliable prediction of droplet spraying (atomization) parameters plays an important part. Such a prediction becomes difficult when the structure of gas-vapor-droplet flows changes due to the interaction of liquid fragments in different interaction modes [7, 8]: bounce, separation, coalescence, and disruption. Thus, it is necessary to take into account the characteristics of these modes when designing plants and developing liquid atomization technologies. Spraying of highly inhomogeneous liquid compositions is often complicated by molecular interactions, micro-explosions, as well as

* Corresponding author, e-mail: piskunovmv@tpu.ru

partial or full dispersion [9]. Therefore, we need to generalize the experimental data for both homogeneous and highly heterogeneous droplets. Regrettably, despite the scientific community's vast experience in researching the interaction of finite solid particles and liquid droplets (in a wide range from 10 μm to 5 mm), the previous processes remain understudied [1-3].

Experimental findings and mathematical models simulating liquid droplet collision in a gas are usually presented in the form of the so-called interaction mode maps [1-3]. These maps are created in the axis systems with due consideration of the Weber number variations, as well as angular and linear parameters of interaction (for impact angle measurement and for studying the role of the impact parameter – the distance between the droplets' centers of mass) [1-3]. For multi-component droplets, interaction mode maps usually consider the Weber, Reynolds, Laplace, Ohnesorge, and capillary numbers, characterizing the correlation of forces of inertia, surface tension, and viscosity [10-12]. Thus, it is underlined [10-12] that the Weber number is not the only criterion define the stability of a homogeneous or heterogeneous droplet colliding with the neighboring ones. Over the recent years, researchers have focused more on the mechanisms of droplet deformation, dispersion, fragmentation, and breakup, which are instrumental in spraying technologies [8, 13].

Of the many parameters describing droplet interaction that are studied experimentally and theoretically [7, 8], of the greatest interest are the interaction time, threshold and transient conditions, as well as the number and size of the post-collision liquid fragments. For instance, values for these parameters are provided in [5, 6]. From the analysis of studies [14, 15], we can conclude that the scientific community has been focusing on recording the duration (typical times) of droplet coalescence. No experimental data or calculations based on modelling of collision times for droplet bounce, separation, or disruption have been published so far. According to studies [14-18], these times are short and cannot differ significantly in such collision behaviors. Experimental data on the quantity and size of liquid fragments formed due to collisions is also scarce. This factor may be instrumental in secondary atomization technologies just as breakup due to overheating of the low boiling component in heterogeneous droplets [5, 6], for instance, in emulsions or more complex (multi component) compositions containing solid particles and liquid additives to water. Surface tension and viscosity of the main liquid and various additives, used to improve the environmental and energy performance of the technologies [19], as well as interfacial tension and intermolecular forces may have a significant effect.

Most of the chemical, heat and power, and fuel gas-vapor-droplet technologies employ droplet collision, usually at different temperatures [5, 6]. Therefore, it is sensible to study the impact of this factor on the interaction time and number of post-collision droplets not only for water but also for typical water-based slurries, emulsions, and solutions. The role of phase transformation can be explored in more detail if we factor in the variation of liquid properties as a function of temperature. As indicated in [20], the incoming droplet (projectile) may be significantly affected by the gas-flow field around the main droplet (target). This is especially noticeable in the bounce mode. Due to phase transformations, this field will change significantly [21], since a vapor-air cushion will emerge between droplets. Its impact on droplet interaction has yet to be studied in full [21]. At a first approximation, it is sensible to compare the experimental results for droplets of liquids, solutions, emulsions, and slurries with different initial temperatures to obtain an understanding of the differences between the interaction times of homogeneous and heterogeneous liquid fragments colliding in a gas.

The purpose of this research is to explore the relationships of bounce, separation, coalescence, and disruption times of liquid droplets *vs.* all the main parameters important for gas-vapor-droplet applications.

Experimental procedures

Experimental set-up and methods

The set-up generated two flows of droplets with fixed dimensions and velocities, while automatically tracking and recording them. The generator capillaries were located at a fixed angle to each other to vary the known dimensionless interaction parameters (β and B) in a wide range from 0-1 [1-3]. Droplet generator nozzles moved with the help of specialized fasteners and mobile set-up elements. Droplet radii ranged from 0.1-5 mm, velocities varied within 0.1-10 m/s, and collision angles were from 0-90°. We used two high speed video cameras (recording frequency up to 10000 fps) focusing on one observation area to obtain 3-D images of colliding droplets.

The systematic errors of radii, R_d, and velocities, U_d, measurement using video recording and the TEMA AUTOMOTIVE software package did not exceed 1.6% and 2.1%, respectively. The maximum random errors of such measurements (due to droplet surface transformations) were $R_d = 2.1\%$, $U_d = 3.4\%$. The systematic error of α_d measurements did not exceed 2.3%, considering the resolution of the video cameras.

The values of B, β, Weber, Reynolds, and Ohnesorge numbers were calculated according to the methods presented in [1-3]. Interaction mode maps (for bounce, separation, disruption, and coalescence) were produced in the B(We), β(We), We(Oh), Re(Oh) co-ordinate systems. To calculate the geometrical (linear) interaction parameter, B, we used the ratio of the impact parameter to the sum of droplet radii: $B = b/(R_{d1} + R_{d2})$ [1-3]. The angular interaction parameter, β, was derived from the impact angle: $\beta = \cos(\alpha_d)$ [1-3]. The parameters β and B define the droplet interaction kinetics because take into account droplets motion vectors, their dimensions, and distances between centers of mass. The values $B = 0$ are typical of conditions of the coaxial collision. In the case when $B = 1$ the collisions happen tangentially under different impact angles. The impact angle value governs the parameter, β. In particular, at $\beta = 0$ the droplets interact at the right angle. When $\beta = 1$, the coaxial collision occurs. For the mode maps, we calculated the Weber numbers of the droplets closing in before collision with due consideration of their relative velocities: $We_1 = 2\rho R_{d1} U_{rel}^2/\sigma$, $We_2 = 2\rho R_{d2} U_{rel}^2/\sigma$ [1-3]. The relative velocity, U_{rel}, of co-directional droplet movement was defined as the difference of U_{d1} and U_{d2}. When the droplets collided head-on, the U_{rel} was calculated as the sum of U_{d1} and U_{d2}. At $\alpha_d = 90°$, we used the value of only one of the velocities for the, U_{rel}, calculation (in line with numerous studies considered in review papers [1-3]. Similar assumptions were made when calculating the Reynolds and Ohnesorge numbers for the colliding droplets under study. The former was calculated to take into account the inertial force to viscosity force ratio and the latter, for viscosity force to surface tension ratio.

It is important for practical purposes to explore surface transformation and collision patterns of heated and evaporating droplets. With that in mind, our experiments were conducted at various droplet temperatures within the range of 20-80 °C typical of gas-vapor-droplet technologies. The lower limit is the liquid spraying temperature in most irrigation technologies and the upper one corresponds to the maximum possible temperature of droplets of liquid compositions based on water used in various heat and mass transfer plants [21]. Volkov *et al.* [21] used non-contact techniques based on particle image velocimetry, laser induced phosphorescence, and planar laser induced fluorescence to establish the temperature fields of droplets of water and various water-based compositions (slurries, solutions, and emulsions) exposed to convective, radiative, and conductive heating. The droplet heating and cooling rates as well as their maximum temperatures (as a rule, 70-80 °C) established in [21] can be regarded as the most valuable result of those experiments. With this in mind, when planning the experiments, we chose the

droplet heating temperature range before their spraying from capillaries and collisions. The examined liquids were heated in a specialized 100 ml tank equipped with small heating coils and a temperature indicator. The droplet temperature and cooling before collision were measured in preliminary experiments conducted using the methods described in [21]. The systematic errors of liquid temperature measurement were 2-3 °C.

Materials

The liquid compositions to be studied were chosen from those widely used in thermal water treatment, heat carriers based on flue gases, water vapor and droplets, secondary atomization of homogeneous and highly inhomogeneous liquids*, etc.* It was also important to compare the experimental results with the data in [14-18] in certain variation ranges of the Weber numbers and interaction parameters. We used the following compositions: tap water, saline solutions (mass fraction of NaCl up to 5 wt.%), oil-in-water emulsions (volume concentration of oil up to 10 vol.%), compositions based on foaming agents (typically used in firefighting for the atomization of water batches discharged), and graphite-water slurries (solid particle concentration up to 5 wt.%). Slurries based on bentonite (key additive inhibiting the growth of spray zone size in firefighting). Table 1 lists the main specifications of liquid compositions under study [12, 22, 23].

Table 1. Characteristics of liquid compositions for the heating temperature range of 20-80 °C (based on [12, 22, 23]; the values for 20 °C are presented and then the sign → demonstrates the characteristics at 80 °C)

Components	Mass [wt.] or volume [vol.] fraction of additive [%]	Density [kgm^{-3}]	Dynamic viscosity [Pa·s]	Surface tension [Nm^{-1}]
Water	–	998 → 965	0.0014 → 0.00036	0.07269 → 0.06259
NaCl solution	5 (wt.)	1147 → 1114	0.0011 → 0.00046	0.08255 → 0.07254
Oil-water emulsion	10 (vol.)	989 → 956	0.00125 → 0.0006	0.0673 → 0.0572
Graphite-water slurry	5 (wt.)	1030 → 997	0.0011 → 0.00046	0.07269 → 0.06259
Foaming agent emulsion	5 (vol.)	1100 → 1047	0.001 → 0.00036	0.023 → 0.0129
Bentonite slurry	5 (wt.)	1030 → 997	0.0011→0.00046	0.072 → 0.069

Parameters of droplet interaction

Apart from the main registered parameters of droplets closing in before contact (section *Experimental set-up and methods*) and component composition of liquids (section *Materials*), we measured the key characteristics of the collision process: interaction time, number and size of post-collision droplets, and the total liquid surface area.

To measure the number of droplets before and after collision as well as to calculate their total surface area, we used custom tracking algorithms by TEMA AUTOMOTIVE. Before collision, we calculated the midsection areas, S_m, of the interacting droplets (for non-spherical shapes, we averaged the four values of S_m for different droplet sections). The formula for the average size calculation was chosen based on the droplet shape. For instance, using $R_d = (S_m/\pi)^{0.5}$, we calculated the average droplet radius. After that, the total areas of the free surface of primary droplets were given by $S = 4\pi R_d^2$. Before contact, the initial liquid surface area, S_0, was equal to the sum of the projectile and target droplet areas. Post-collision liquid

fragments had different shapes and dimensions, which made them difficult to analyze in detail. Therefore, we assumed all the resulting (mostly small-sized) fragments to be spherical. In this case, we calculated the mean radii of the fragments and their surface areas using Tema Automotive and then added them together. The total surface area of all the liquid droplets were calculated after the two primary ones collided, S_1.

There are four droplet collision behaviors, which we recorded: coalescence, bounce (droplets close in and interact through a gas cushion, which they cannot break through due to the lack of kinetic energy), separation (droplets collide to form two post-collision droplets with radii similar to the primary ones), and disruption (droplets atomize or break up completely). For each of these behaviors, we calculated dimensional, t, and dimensionless, τ, durations of interaction. Dimensionless values of times were given by $\tau = U_{rel}t/2R_d$ [14]. The coalescence time, t_c, was the interval between the contact of colliding droplets and the formation of a singular droplet with stable geometry (no fragments). The separation time, t_s, and bounce time, t_b, were calculated from the point of closest approach of the droplets followed by their separation until the distance between them became equal to the radius of the smallest one of the two droplets (*i.e.*, one typical size of the small colliding object). The disruption time, t_d, was defined as the time between the contact of the two colliding droplets and the formation of a finite number of satellite droplets (usually no less than 10). The accuracy of t_c, t_s, t_b, and t_d calculation largely depended on the recording frequency and resolution of the high speed cameras. The maximum allowable error was set as 10^{-4} second. The recording frequency ranged from 10000-50000 fps, depending on the collision behavior, droplet size and the region of the observation area occupied by the newly formed liquid fragments (*i.e.*, we calculated their number and the S_1/S_0 ratio). The τ estimation accuracy was affected by the accuracy of U_{rel} as well as projectile, R_{d1}, and target, R_{d2}, droplet size measurement.

Results and discussion

Droplet collision behaviors and patterns

Figure 1 shows the water droplet interaction times under ambient conditions (at 20 °C) *vs.* the Weber number. It also gives typical values of t_c, t_s, t_b, and t_d on the so-called interaction mode maps, *i.e.*, when the linear and angular parameters as well as inertial forces and surface tension are varied (We, β, B). Figure 1(a) reveals a general pattern that the interaction times are the shortest in the disruption mode. Separation takes somewhat longer, whereas the longest times are observed for coalescence, closely followed by bounce. These patterns come from the aerodynamic forces acting on the droplets in the corresponding collision mode in the specified Weber number ranges. In particular, disruption is stable at We > 50, *i.e.*, when inertial forces dominate surface tension. Minimum Weber numbers are typical of bounce and coalescence, in particular, bounce was observed at We < 2, and coalescence at up to We = 30. Then the separation started to dominate (as a rule, We = 30-50). Figures 1(b) and 1(c) shows that the interaction modes and times of the corresponding collision behaviors are determined by not only the Weber numbers but also the main interaction parameters: angular, β, and linear, B. The interaction times in the mode maps confirm the instrumental contribution of the interaction kinetics. In particular, at a zero impact angle and opposite motion directions of droplets, the time of their collision is minimum in each of the modes under study. Co-directional movement (the second droplet followed the first one until collision) provides the longest interaction times. At 15-80°, average collision times are observed. This mostly results from a change in the interaction mode from the dominating disruption or bounce to separation or coalescence, respectively.

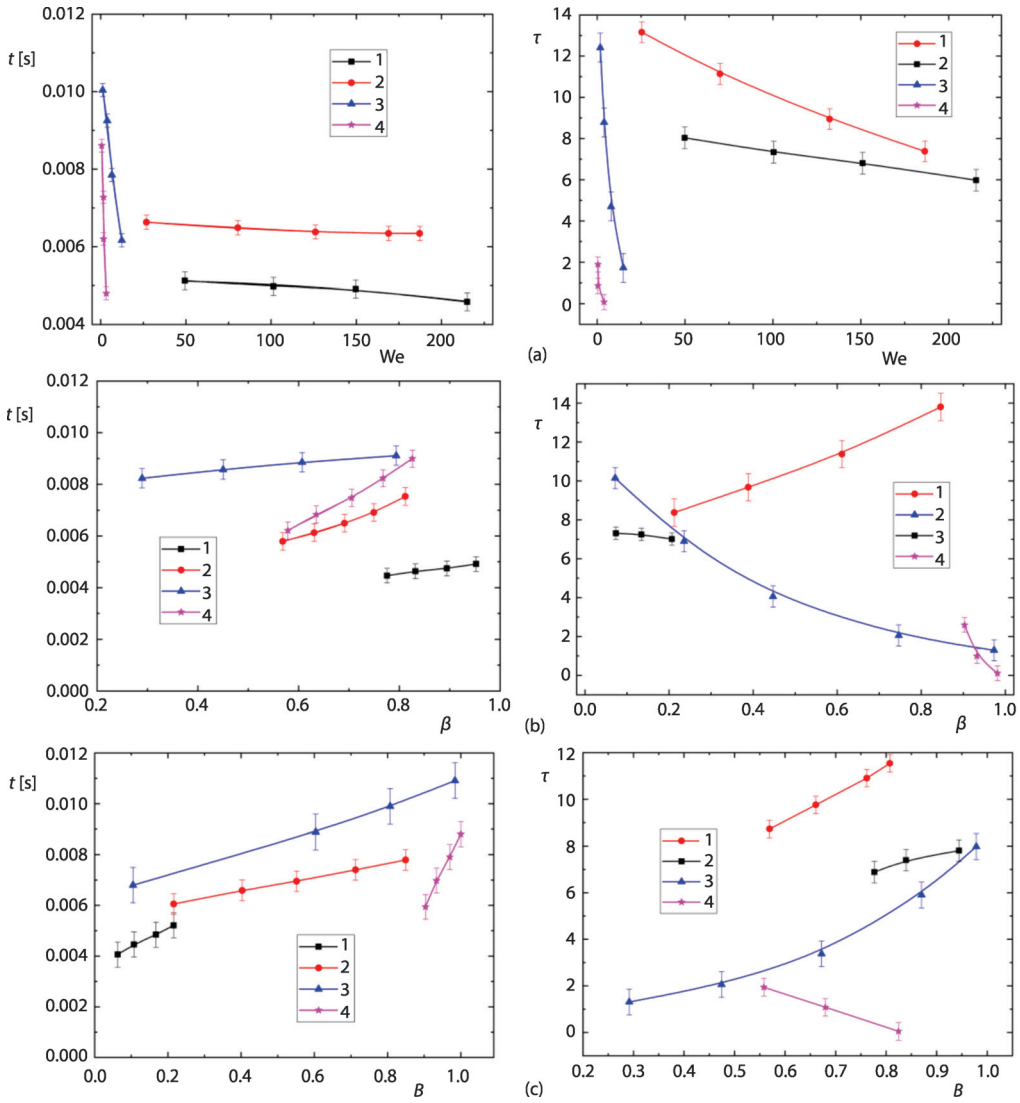

Figure 1. Dimensional and dimensionless droplet interaction times *vs.* the Weber number (*a*), angular interaction parameter (*b*), and linear interaction parameter (*c*) in different modes: *1 – disruption, 2 – separation, 3 – coalescence, and 4 – bounce*

The analysis of dimensionless droplet interaction mode maps shows that we can also reliably produce interaction time maps to show dimensional, t, and dimensionless, τ, collision times *vs.* β, B, and We. Local increases or decreases in dimensional times observed in the experiments are not always noticeable when the interaction times become dimensionless. Hence, it is important to demonstrate different variation rates of t and τ.

We have established that at $\beta \rightarrow 1$ the interaction times are the longest in the bounce and coalescence modes and the shortest for disruption and separation. At $\beta \rightarrow 0$, the times of all the interactions are minimum, because the interaction rate of droplets is defined by the velocity

of the projectile droplet. At the same time, of all the modes, the weakest relationships are of droplet coalescence and disruption times *v*s. β.

The times of all the four modes are significantly affected by the parameter B. The higher it is, the more significantly the droplet interaction times grow, especially in the coalescence mode, fig. 1. This pattern stems from the fact that parameter B characterizes the distance between the droplets' centers of mass. The smaller this distance, the more intense the droplet interaction (the collisions are almost coaxial, and the droplet contact area is rather large). At lower values of B, grazing collisions of droplets become more frequent. These provoke significant droplet transformation, swirling, and rotation of both fragments after collisions, which prolongs the droplet interaction times in all the modes. We observed different growth rates of t and τ as functions of B, but in all cases, they can be described by a power function of the second order, as shown in fig. 1. As suggested by the nature of droplet surface transformations, the most noticeable changes are observed for coalescence and bounce, fig. 1.

Figure 1 clearly shows the variation ranges of β, B, and We, in which we can use approximations to show the single-factor impact on interaction times, for instance, $\tau(\beta)$, $\tau(B)$, or τ(We), as well as regions requiring complex 2-D or even 3-D co-ordinate systems controlling for the simultaneous impact of β, B, and We. Further, we will demonstrate that the number of decisive factors increases significantly in the case of multi-component compositions. It is sensible to take into account the Ohnesorge and Reynolds numbers criteria for estimating the correlation of viscosity force (internal friction) as well as surface tension and inertia forces.

At a small impact angle, droplets break up to form fine aerosol, so, with an increase in the impact angle (or decrease in β), the time of droplet disruption is reduced. The trajectories of colliding droplets coincide but the directions are opposite to each other. The interaction rate, *i.e.*, the rate of droplet coalescence goes down due to the opposing motion vectors of the droplets. At a non-zero impact angle, the projectile does not hit the exact center of the target (*non-coaxially* or *off-center* are popular terms), so droplets break up to form a bridge between them. The relative droplet velocity does not change much (droplets do not slow down noticeably when closing in), so the disruption process is faster and more dynamic, with more small-size liquid fragments formed as a result.

The coalescence time of liquid fragments increases significantly with an increase in the relative linear interaction parameter B, describing the ratio of the distance between the droplets' centers of mass and the sum of their sizes. This effect is connected with the increasing impact of droplet dimensions. The larger the dimensions, the longer time it takes for a new droplet to reach a stable shape.

Impact of relative droplet velocity and size correlation

When analyzing how much the correlation of droplet size and relative velocity affects the interaction times, we established that the scale of impact differs greatly from one liquid composition another. In some cases, coalescence and bounce times become even shorter than those of separation and disruption. These patterns clearly illustrate the countervailing influence of several factors ignored when calculating droplet interaction times as functions of only size or relative velocity correlation. If we compare figs. 1 and 2, we see complex-looking curves of dimensionless droplet interaction times, τ, unlike similar functions of dimensional times, t. Droplet size and velocity that are part of the expression for time, τ, have a different-scale impact on the liquid fragment collisions. These effects become especially noticeable when plotting the curves of τ *vs*. β and B, since the latter reflect the kinetics of collision related to both droplet size and velocity.

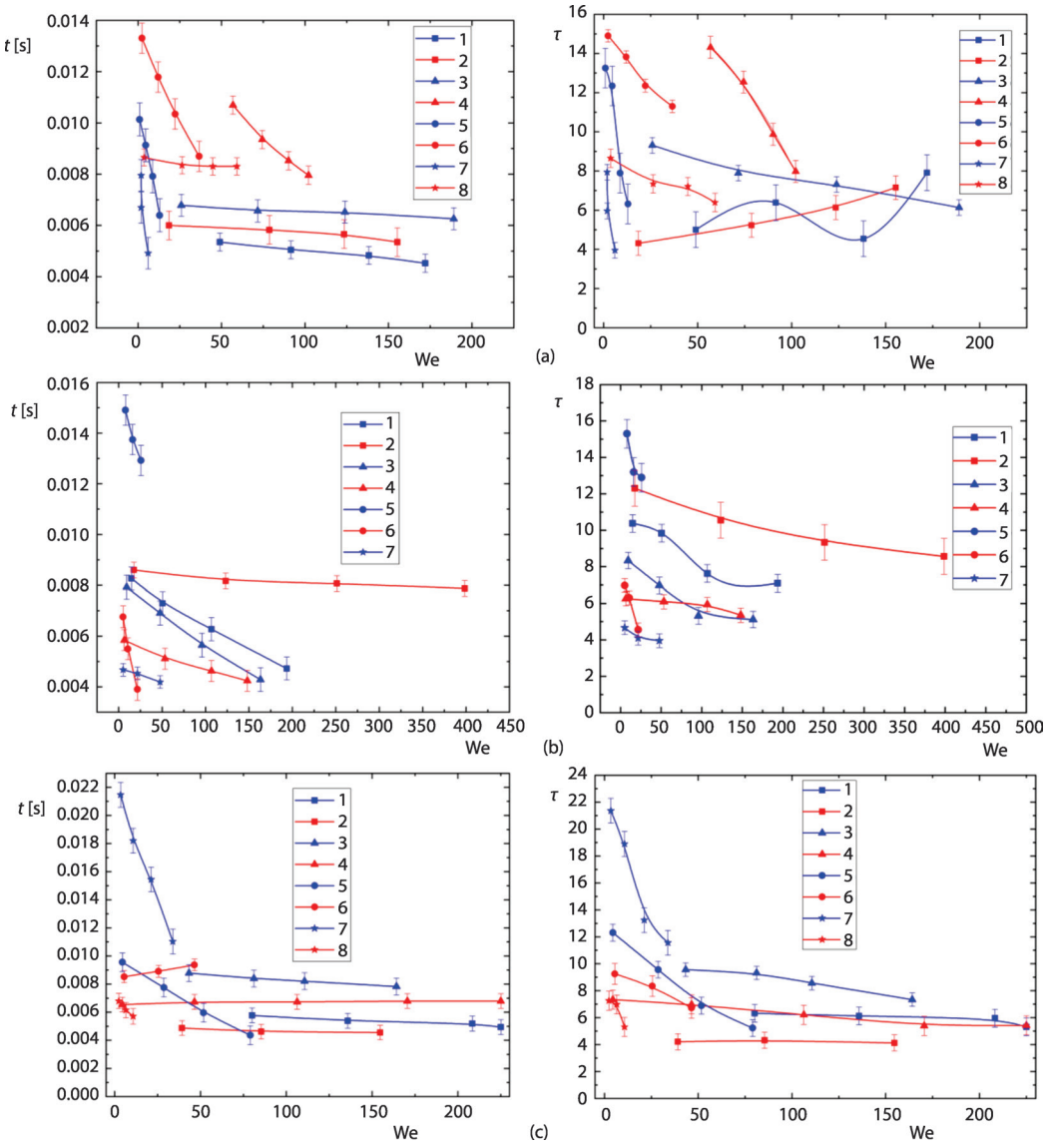

Figure 2. Dimensional and dimensionless droplet interaction times; (a) water, (b) slurry, and (c) emulsion, *vs.* Weber numbers at various liquid temperatures, compositions at 20 °C are marked in blue and those at 80 °C, in red: *1, 2 – disruption, 3, 4 – separation, 5, 6 – coalescence, and 7, 8 – bounce*

Looking at figs. 1 and 2, we can conclude that the dimensionless time, τ, has strong limitations to its applicability for studying the physics of liquid fragment interaction. Weber number established quite a good agreement between the nature of the curves for t and τ as functions of Weber number only. However, in some experiments, we recorded the same values of Weber number in the collision area by different-sized droplets with different velocities. This factor led to an increase in the experimental data dispersion despite the identical Weber number values and to non-monotonous variations of τ values, *e.g.*, fig. 2(a) and 2(b) shows this effect

for several curves. Therefore, we can conclude that the τ(We) or t(We) functions alone are not enough to describe the variation dynamics of droplet collision time t. It is important to take into account more factors and effects and make an attempt to describe their contribution using approximations.

Impact of droplet temperature

Quite interesting are the results obtained by exploring how droplet heating affects droplet interaction times, fig. 2. Significant changes are observed in critical Weber number values (transient between various interaction modes) as well as bounce and coalescence times as functions of Weber number at various droplet temperatures, fig. 2. Moreover, the shape of the curves change considerably as well.

Figure 2 clearly shows that for almost all the interaction modes and compositions, times t and τ go up with an increase in the liquid droplet temperature. When the droplet temperature rises, the surface tension and viscosity are supposed to decrease. Hence, less energy is required to surmount the repulsive forces, and the interaction should take less time. However, the values of t and τ in fig. 2 show the opposite effect, especially noticeable in the coalescence and bounce modes. This may be explained by the presence of not only a gas cushion but also a vapor one between the colliding droplets due to phase transformations. The higher the droplet temperature, the more noticeable the effect. The emergence of a vapor cushion layer between droplets leads to an increase in the kinetic energies of liquid fragments required for collision. Experimental results [24] show that heating and evaporation rates of heterogeneous droplets are significantly higher than those of single-component ones. This is what causes more considerable variations of coalescence and bounce times for heated heterogeneous droplets of slurries and emulsions as compared to water and other compositions, fig. 2.

In actual gas-vapor-droplet technologies based on heat and mass transfer, droplet surface and gas-vapor mixture temperature around them may be much higher than in our experiments. Therefore, the role of vapor cushion around droplets will be more significant than pointed out in the analysis of fig. 2. Linear vapor velocities may reach 0.1-0.3 m/s [25]. Typical relative velocities of bouncing droplets do not exceed 0.7 m/s. As a result, the maximum relative interaction rates of droplets in the bounce mode may differ by 30-40%. This has a significant impact on the interaction time of colliding liquid fragments.

Impact of droplet component composition

In the case of solutions, emulsions, and slurries, it is sensible to study the impact of component composition with due consideration of the two key parameters: surface tension and viscosity of the liquid. Hence, we can obtain the droplet interaction times of liquids, solutions, emulsions, and slurries as functions of these two parameters or dimensionless criteria, *e.g.*, the Reynolds, Ohnesorge, and Weber numbers. Figures 3 and 4 show the impacts of these factors in our experiments as well as comparisons with the experimental data from [14].

As can be seen in figs. 3 and 4, the impact of surface tension and viscosity of the liquids on interaction times is quite obvious. An increase in the surface tension causes a highly non-linear decrease in interaction times, whereas the growing viscosity prolongs these times. However, such trends are not observed for all the modes, (see figs. 3 and 4. In particular, disruption times become longer with an increase in viscosity, since the aerosol is formed rather quickly, *i.e.*, newly formed liquid fragments have a short relaxation time.

The shape of the curves presented in fig. 3 is in good agreement with experimental data and conclusions from [14-18]. With higher surface tension and lower viscosity of the liquid

composition, more kinetic energy of the droplets is required for their significant transformation and breakup. Hence, with higher surface tension and lower viscosity of the composition, droplets will separate at somewhat higher velocities or droplet dimensions. This causes droplets to collide and break up much faster, figs. 3 and 4. Droplet coalescence or separation times become much longer in figs. 3 and 4, since increased liquid viscosity strengthens molecular bonds.

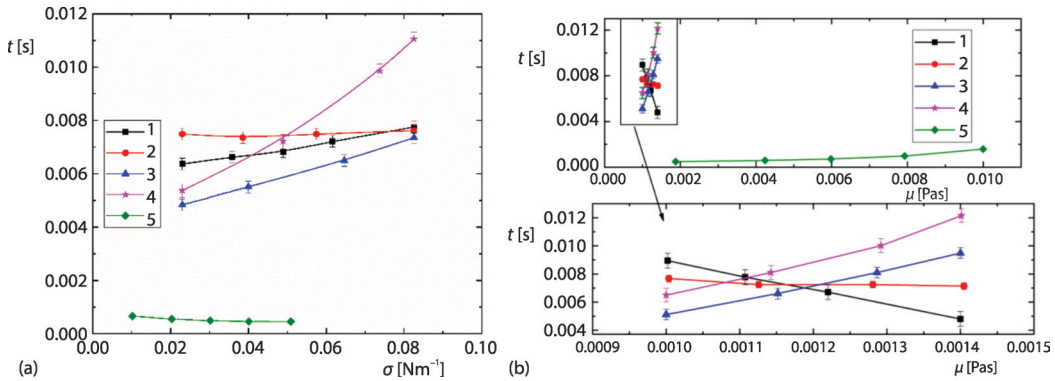

Figure 3. Interaction times of droplets of liquid compositions under study for different collision behaviors (*1 – disruption, 2 – separation, 3 – coalescence, 4 – bounce, and 5 – data from [14]*) *vs.* surface tension (*a*) and viscosity (*b*)

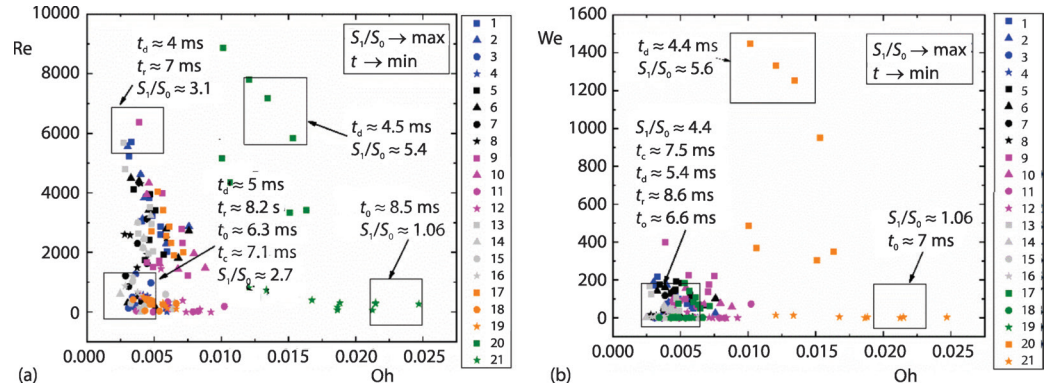

Figure 4. Interaction mode maps factoring in Ohnesorge and Reynolds numbers (a) and Weber number (b) with typical droplet collision times: water: *1 – disruption, 2 – separation, 3 – coalescence, 4 – bounce,* graphite-water slurry, *5 – disruption, 6 – separation, 7 – coalescence, 8 – bounce;* oil-water emulsion, *9 – disruption, 10 – separation, 11 – coalescence, 12 – bounce, 13 – disruption; saline solution, 14 – separation, 15 – coalescence, 16 – bounce,* foaming agent emulsion, *17 – separation, 18 – coalescence, 19 – bounce, b*entonite slurry, *20 – disruption, and 21– bounce*

If we explore the differences between the droplet interaction modes for water and water-based slurries, solutions, and emulsions, we will see that the dominating collision outcomes of slurry droplets are separation and disruption and for emulsions, it is coalescence and disruption. Droplets of solutions and water are observed in all the four interaction modes, figs. 3 and 4. A wide variation range is established for water droplet interaction times.

The most valuable findings of the research into heterogeneous droplets seem to be the interaction mode maps of We(Oh) and Re(Oh), fig. 4, with the variation rates of typical droplet interaction times and S_1/S_0. This ratio shows how the liquid surface area changes after the drop-

lets collision, S_1, compared to the initial one, S_0. These mode maps make it possible to generalize experimental data for various droplet compositions and applications. From figs. 1 and 4 we can conclude that the impact of all the factors and processes under study on droplet interaction times can be best described using the complex expressions, τ (We, Re, Oh, B, β), which are, however, extremely resource-intensive. Therefore, a high potential objective would be to establish the variation ranges of parameters, for which 2-D interaction mode maps can be used.

The most challenging task is to reliably predict the collision outcomes of slurry droplets. According to the analysis of video frames, solid particles concentrate in one of the droplet parts due to different densities. Therefore, the kinetic energy of a slurry droplet is higher than that of a water droplet. These factors cannot be described even in a multi-dimensional factor space, *e.g.*, τ (We, Re, Oh, B, and β). In this case, it will be necessary to study the impact of slurry sedimentation before collisions. These effects are not that important for solutions and emulsions, because they retain their stable structure for a longer time.

Evaluation of minimum disruption times and degree of atomization

Based on the videoframes, the typical collision outcomes of compositions under study differ significantly in the number and dimensions of the post-collision liquid fragments and the total area of their surface. The difference in the quantity of liquid fragments and their dimensions is especially noticeable between the disruption and separation modes. Slurry droplets broke up into the greatest number of fragments of the smallest size followed by emulsion, solution, and water droplets in the order of numerical values. Despite the differences in the bonding energies of Na^+ and Cl^- from those of water molecules, the characteristics of newly formed fragments differed negligibly (within the experimental error). For slurry droplets, an increase in the number of post-collision fragments results from the unstable surface (due to the heterogeneous composition and different component densities) as well as the hydrophilic and hydrophobic effects encouraging small water batches to follow the solid particles breaking away from the surface.

Figures 4 and 5 show the S_1/S_0 ratios as functions of Weber, Reynolds, and Ohnesorge numbers, B, and β. The impact of each of these parameters on the growth of the total droplet sur-

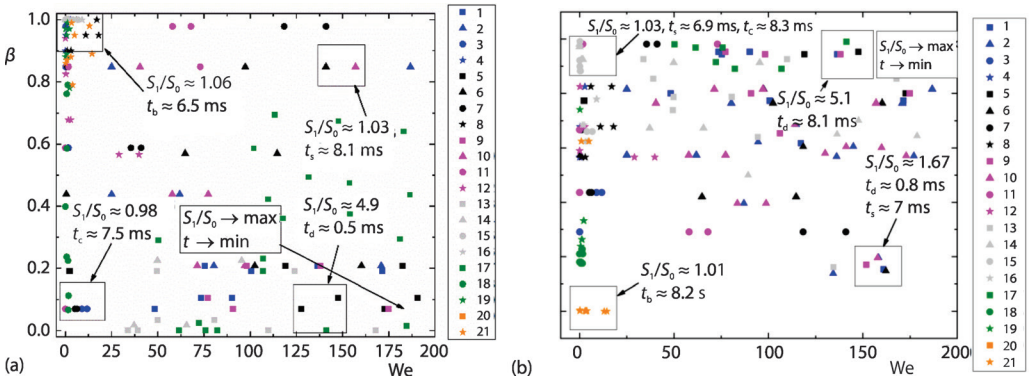

Figure 5. Values of S_1/S_0 on collision behavior maps produced using dimensionless angular (*a*) and linear (*b*) interaction parameters; water: *1 – disruption, 2 – separation, 3 – coalescence, 4 – bounce,* graphite-water slurry, *5 – disruption, 6 – separation, 7 – coalescence, 8 – bounce;* oil-water emulsion, *9 – disruption, 10 – separation, 11 – coalescence, 12 – bounce; saline solution: 13 – disruption, 14 – separation, 15 – coalescence, 16 – bounce,* foaming agent emulsion, *17 – separation, 18 – coalescence, 19 – bounce,* bentonite slurry, *20 – disruption, and 21– bounce*

face area is quite clearly visible and so are the conditions limiting the variation of S_1/S_0. In this research, we have, for the first time, established the conditions that can provide maximum values of S_1/S_0 with minimum interaction times (τ and t) in the corresponding modes, figs. 4 and 5. These conditions are instrumental for understanding how droplet atomization can be intensified with limited time and resources available.

The experiments provided us with the necessary experimental database. This can be used to formulate the adjusting coefficients to develop droplet interaction models with due consideration of interaction rates and times, see the overview in [1-3]. Several reliable models of this kind will help optimize liquid spraying parameters in gas- and vapor-droplet technologies [26], where it is especially important to control and predict the gas-vapor-droplet composition. These include thermal and flame water treatment [27], heat exchange technologies of evaporation and condensation in heat and power ducts, units, and blocks [28]. Heat carriers from flue gases, water droplets and vapors [29]. Ignition of composite fuels without injector clogging or jet fading in combustion chambers [30]. Temporally and spatially distributed gas-vapor-droplet mixture supply to combustion zones for the effective fire containment and suppression [31]. One of the numerous practical applications of the experimental results is the atomization of liquid and slurry fuels in internal combustion engine chambers or in power plant furnaces to improve their performance. Droplet interaction times (3 ms < t < 10 ms) in the four possible interaction modes are comparable to the duration of one combustion engine cycle and one ignition cycle in boiler units (several ms). Thus, the secondary atomization of fuel droplets in such units can only be optimized if the aforementioned factors are taken into account. For instance, the right conditions for the secondary atomization of slurry, emulsion and liquid fuels should be chosen to avoid coalescence, bounce, and separation, and to intensify disruption. Moreover, fuel spraying conditions should provide maximum S_1/S_0 values and minimum disruption times based on the fuel properties, combustion chamber geometry, and engine operation conditions.

Conclusions

- The experiments allowed us to explore the impact of a large set of factors (relative velocity, size, impact angle, impact parameter, temperature, component composition of droplets*, etc.*) on the typical bounce, disruption, coalescence, and separation times. Approximation equations of τ and t as functions f(We), f(Re), $f(\beta)$, and $f(B)$ were obtained with due consideration of dimensional and dimensionless droplet interaction times. Almost all the factors and effects under study were found to have a large-scale impact on interaction times. This way the atomization process could be controlled, changing the general trend that disruption lasted the shortest time followed by the times of separation, bounce, and coalescence. However, the rapid evaporation of heated droplets caused an increase in the times τ and t in the bounce and coalescence modes.
- The experimental results and approximation equations develop the numerous earlier experimental and theoretical studies in this field. For the first time, droplet interaction times were measured in all the four collision outcomes. We determined the conditions of $t \rightarrow$ min and $S_1/S_0 \rightarrow$ max with due consideration of the available collision mode maps based on β, B, Weber, Reyolds, and Ohnesorge numbers. It is difficult to provide such conditions for the dimensionless time τ, since not only the time t, but also droplet size and velocity play a decisive role. The experimental parameters were in line with the high potential gas-vapor-droplet technologies, such as thermal water treatment, heat carriers based on flue gases, water vapor and droplets, as well as miscellaneous heat and mass transfer plants.

- The established functions of droplet interaction times promote the powder technology by improving and supplementing the current models used to describe changes in the structure and composition of droplet aerosols. It is sensible to continue this research and study the collisions of highly heterogeneous droplets in multi-phase and multi-component flows. In this case, it will be possible to obtain more exact $f(\sigma)$, $f(\mu)$, f(We), and f(Re)*, etc.*

Acknowledgment

This study was funded by Russian Science Foundation (Grant No. 18-71-10002).

Nomenclature

b – distance between droplets' centers of mass, [mm]
B – dimensionless linear interaction parameter (= $b/(R_{d1} + R_{d2})$, [–]
B_1, – dimensionless constants in approximations, [–]
Oh – Ohnesorge number (= $\mu(\sigma\rho^2 R_d)^{1/2}$, [–]
R_{d1} – first droplet radius, [mm]
R_{d2} – second droplet radius, [mm]
Re – Reynolds number (= $\rho^2 R_d U_{rel}\mu^{-1}$), [–]
S_0 – initial liquid surface area, [mm^2]
S_1 – total surface area of all liquid droplets after collision of two primary droplets, [mm^2]
S_m – frontal cross-sectional area of colliding droplets, [mm^2]
t – interaction time, [s]
t_b, t_c, t_d, t_s – duration of bounce, coalescence, disruption, and separation, [s]
U_{d1} – first droplet velocity, [ms^{-1}]
U_{d2} – second droplet velocity, [ms^{-1}]
U_{rel} – relative droplet velocity, [ms^{-1}]
x, y – functions in approximations, [–]
We – Weber number (= $2\rho R_d U_{rel}^2/\sigma$), [–]

Greek symbols

α_d – impact angle, [°]
β – dimensionless angular interaction parameter [= $\cos(\alpha_d)$], [–]
μ – dynamic viscosity, [Pa·s]
ρ – density, [kgm^{-3}]
σ – surface tension, [Nm^{-1}]
τ – dimensionless interaction time (= $U_{rel}t/2R_d$), [–]

References

[1] Orme, M., Experiments on Droplet Collisions, Bounce, Coalescence And Disruption, *Prog. Energy Combust. Sci*., *23* (1997), 1, pp. 65-79
[2] Krishnan, K. G., Loth, E., Effects of Gas and Droplet Characteristics on Drop-Drop Collision Outcome Regimes, *Int. J. Multiph. Flow*, *77* (2015), Dec., pp. 171-186
[3] Pawar, S. K., *et al*., An Experimental Study of Droplet-Particle Collisions, *Powder Technol.*, *300* (2016), Oct., pp. 157-163
[4] Li, X., *et al*., Effect of Ambient Temperature on Flash-Boiling Spray Characteristics for a Multi-Hole Gasoline Injector, *Exp. Fluids*, *60* (2019), 7, pp. 109
[5] Vysokomornaya, O. V, *et al*., Breakup of Heterogeneous Water Drop Immersed in High-Temperature Air, *Appl. Therm. Eng*., *17* (2017), 30338-1, pp. 1359-4311
[6] Strizhak, P.A., et al., Evaporation, Boiling And Explosive Breakup Of Oil–Water Emulsion Drops Under Intense Radiant Heating, *Chem. Eng. Res. Des*., *127* (2017), Sept., pp. 72-80
[7] Zhang, H., *et al*., Study on Separation Abilities of Moisture Separators Based on Droplet Collision Models, *Nucl. Eng. Des*., *325* (2017), Dec., pp. 135-148
[8] Finotello, G., *et al*., Experimental Investigation of Non-Newtonian Droplet Collisions: The Role of Extensional Viscosity, *Exp. Fluids*, *59* (2018), 7, pp. 113
[9] Moussa, O., *et a*l., Parametric Study of the Micro-Explosion Occurrence of W/O Emulsions, *Int. J. Therm. Sci*., *133* (2018), Nov., pp. 90-97
[10] Wang, Y., *et al*., Events and Conditions in Droplet Impact: A Phase Field Prediction, *Int. J. Multiph. Flow*, *87* (2016), Dec., pp. 54-65
[11] Charalampous, G., Hardalupas, Y., Collisions of Droplets on Spherical Particles, *Phys. Fluids*, *29* (2017), 10, pp. 103305
[12] Arkhipov, V. A., *et al*., Stability of Colliding Drops of Ideal Liquid, *Journal Appl. Mech. Tech. Phys*., *24* (1983), 3, pp. 371-373

[13] Murko, V. I., *et al.*, Investigation of the Spraying Mechanism and Combustion of the Suspended Coal Fuel, *Thermal Science*, *19* (2015), 1, pp. 243-251
[14] Mohammadi, M., *et al*., Direct Numerical Simulation of Water Droplet Coalescence in the Oil, *Int. J. Heat Fluid-Flow*, *36* (2012), Aug., pp. 58-71
[15] Zhang, Y., *et al.*, Coalescence of Two Initially Spherical Bubbles: Dual Effect of Liquid Viscosity, *Int. J. Heat Fluid-Flow*, *72* (2018), Aug., pp. 61-72
[16] Krebs, T., *et al*., Coalescence Kinetics of Oil-in-Water Emulsions Studied with Micro-fluidics, *Fuel*, *106* (2013), Apr., pp. 327-334
[17] Gebauer, F., *et al*., Detailed Analysis of Single Drop Coalescence – Influence of Ions on Film Drainage and Coalescence Time, *Chem. Eng. Res. Des*., *115* (2016), Part B, pp. 282-291
[18] Ghaffari, A., Hashemabadi, S. H., Parameter Study and CFD Analysis of Head on Collision and Dynamic Behavior of Two Colliding Ferrofluid Droplets, *Smart Mater. Struct*., *26* (2017), 3, 35010
[19] Nyashina, G. S., *et al*., Environmental Benefits and Drawbacks of Composite Fuels Based on Industrial Wastes and Different Ranks of Coal, *Journal Hazard. Mater.*, *347* (2018), Apr., pp. 359-370
[20] Jiang, Y. J., *et al*., An Experimental Investigation on the Collision Behaviour of Hydrocarbon Droplets, *Journal Fluid Mech*., *234* (1992), Jan., pp. 171-190
[21] Volkov, R. S., *et al*., Temperature and Velocity Fields of the Gas-Vapor Flow Near Evaporating Water Droplets, *Int. J. Therm. Sci*., *134* (2018), Dec., pp. 337-354
[22] Shraiber, A. A., *et al*., Deformation and Breakup of Drops by Aerodynamic Forces, *Atomization and Sprays*, *6* (1996), 6, pp. 667-692
[23] Volkov, R. S., *et al*., Water Droplet with Carbon Particles Moving through High-Temperature Gases, *Journal Heat Transfer*, *138* (2015), 1, pp. 014502-014502-5
[24] Antonov, D. V, *et al*., Experimental Study of the Effects of Collision of Water Droplets in a Flow of High-Temperature Gases, *Journal Eng. Phys. Thermophys*., *89* (2016), 1, pp. 100-111
[25] Volkov, R. S., *et al*., Statistical Analysis of Consequences of Collisions between Two Water Droplets Upon Their Motion in a High-Temperature Gas-Flow, *Tech. Phys. Lett*., *41* (2015), 9, pp. 840-843
[26] Ko, G. H., Ryou, H. S., Droplet Collision Processes in an Inter-Spray Impingement System, *Journal Aerosol Sci*., *36* (2005), 11, pp. 1300-1321
[27] Vysokomornaya, O. V, *et al*., High-Temperature Evaporation of Water Emulsion Droplets Used in Thermal Fluid Treatment, *Int. J. Heat Mass Transf*., *126* (2018), Part A, pp. 1043-1048
[28] Legros, J. C., *et al*., Water Drops with Graphite Particles Triggering the Explosive Liquid Breakup, *Exp. Therm. Fluid Sci*., *96* (2018), Sept., pp. 154-161
[29] Voytkov, I. S., *et al*., Temperature Traces of Water Aerosols, Water-Based Emulsions, Solutions and Slurries Moving in a Reversed Flow of High-Temperature Gases, *Exp. Therm. Fluid Sci.*, *98* (2018), May, pp. 20-29
[30] Vershinina, K. Y., *et al*., Ignition of Coal-Water Fuels Made of Coal Processing Wastes and Different Oils, *Appl. Therm. Eng*., *128* (2018), Jan., pp. 235-243
[31] Zhdanova, A. O., *et al*., Suppression of Forest Fuel Thermolysis by Water Mist, *Int. J. Heat Mass Transf*., *126* (2018), Part A, pp. 703-714

Paper submitted: September 28, 2019
Paper revised: December 28, 2020
Paper accepted: April 25, 2021